Journal of
NANOSTRUCTURES
JNS NANOSTRUCTURES
JNS.kashanu.ac.ir

Fabrication and Optical Characterization of Silicon Nanostructure Arrays by Laser Interference Lithography and Metal-Assisted Chemical Etching

Mohsen Nazoktabar[a], Mohamad Zahedinejad[b], Payam Heydari[a,*], Ali Reza Asgharpour[a]

[a]*Faculty of Engineering, Islamic Azad university, Roudehen Branch.*

[b]*Electrical and Computer Engineering Department, University of Tehran*

Article history:
Received 6/10/2014
Accepted 19/11/2014
Published online 21/12/2014

Keywords:
Photovoltaic
laser interference lithography
Metal-assisted chemical etching

**Corresponding author:*
E-mail address:
Pheydari@riau.ac.ir

Abstract

In this paper metal-assisted chemical etching has been applied to pattern porous silicon regions and silicon nanohole arrays in submicron period simply by using positive photoresist as a mask layer. In order to define silicon nanostructures, Metal-assisted chemical etching (MaCE) was carried out with silver catalyst. Provided solution (or materiel) in combination with laser interference lithography (LIL) fabricated different reproducible pillars, holes and rhomboidal structures. As a result, Submicron patterning of porous areas and nanohole arrays on Si substrate with a minimum feature size of 600nm was achieved. Measured reflection spectra of the samples present different optical characteristics which is dependent on the shape, thickness of metal catalyst and periodicity of the structure. These structures can be designed to reach a photonic bandgap in special range or antireflection layer in energy harvesting applications. The resulted reflection spectra of applied method are comparable to conventional expensive and complicated dry etching techniques.

2014 JNS All rights reserved

1. Introduction

Porous silicon has been extensively studied since the discovery of its luminescence properties at room temperature in 1990.The luminescence, high resistivity, large surface to volume ratio, and high chemical activity of porous silicon has resulted in its introduction to many applications such as optoelectronic devices [1,2], gas sensors[3] and humidity sensors[4].

Owing to their structure and mechanical properties, silicon nanowires (SiNWs) and porous silicon have been intensively studied for application in photovoltaic devices [5], energy storage [6], nano-electromechanical systems (NEMS)[7-9], flexible electronics[10] and photonic

devices[11]. Individually, SiNW hierarchical superstructures synthesized by chemical vapour deposition have been considered

for the realization of diodes and transistors [12]. In electronics and in medical science, they used to investigate the behaviour of motor proteins [13] and cell adhesion mechanisms [14]. Specially, several biosensors based on SiNWs have been developed for glucose monitoring [15], multiplexed protein detection [16], label-free DNA detection [17] and single-virus detection [18].

To obtain either porous silicon or SiNWs in an oxidant HF solution, Metal-assisted chemical etching (MaCE) was introduced by Li [19] and Peng [20]. According to this method, our previous research combined regular photoresist mask with MaCE to present a simple and efficient way to pattern porous Si and SiNW arrays with a wide range of porosity levels [21].

In the present work, holes with different periodicities and depth were created in Si wafer by combining laser interference lithography (LIL) and metal-assisted chemical etching for submicron features. LIL includes a simple technique for obtaining a well- defined and large area periodic structure which can generate uniform, sub-micrometer patterns over large areas [22, 23]. Combined MaCE and LIL method is simpler than most conventional dry etching methods which are used to transfer the patterns to fabricate silicon photonic crystal slabs [24].

Reflection spectra for such periodic structures exhibit reflection less than bare Silicon. Furthermore, the structure can be designed to increase the absorption up to 100% [25]. This characteristic makes them interesting substrates for photovoltaic devices and solar cells, specially [26-28].

This method can also be used to fabricate silicon photonic crystals [29] and also, is the promising approach in Si bulk nano-micromachining applications.

2. Experimental procedure

P-type Si (100) with resistivity levels wafers of 285Ω.cm were used in present experiments. After RCA cleaning, all of the samples were covered by Shipley S1400 photoresist.

Nanolithography was performed using interference lithography and a He-Cd laser emitted at325nm to define periods of 1 and 2μm.

The schematic setup of interference lithography is shown in Fig. 1 This setup is able to create feature sizes down to half of the wavelength. The laser beam was separated by a beam splitter (BS) into two beams of equal intensity and passed through two spatial filters to delete speckles. Then, the beams were directed towards the sample to interfere with each other in the photoresist layer coated on the sample.

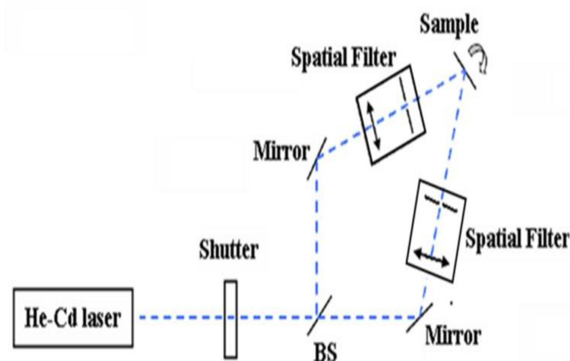

Fig. 1. Schematic of interference lithography setup used for fabrication of photonic crystals

The period of the interference pattern is given by $d = \frac{\lambda}{2 \sin \theta}$, where λ and θ are the laser wavelength and the half angle between the interference beams on the sample, respectively [30]. To fabricate the 2-D PC after the first irradiation step, the sample was rotated and irradiated again. For square shape patterns, the sample was rotated 90° and for the others 83°. We used the optical setup to obtain periodic dots with a period of 1and 2μm. This leads to uncovered silicon areas with feature sizes that are about one half of the period.

2.1 fabrication of photonic crystals

After developing, a thick layer of silver (varying between 15and 30 nm) was deposited on the samples surface using a thermal evaporation system following by the lift- off technique. The deposition rate was kept at 1 Å/s for all thicknesses. The resist layer was then lifted using acetone in an ultrasonic bath. Subsequently, the samples were immersed in etching solution containing 0.4M H_2O_2 and 4.8M HF. After the etching process, the Ag layer was removed by concentrated nitric acid.

Metal nanoparticles act as local cathodes to mediate the reduction of $H_2O_2$and consequently causes the hole injection necessary for the etching reaction.

3. Results and discussion

3.1. Structural investigation of samples after MaCE

Fig. 2(a) shows the distribution of silver nanoparticles that were deposited for 10secondsinsolution containing 4.6 M and 0.005M of HF and $AgNO_3$, respectively, for 600nm period interference lithography.Fig. 2(b) shows an SEM image of the thick silver layer (30nm) after the lift-off process for a 1μm period.

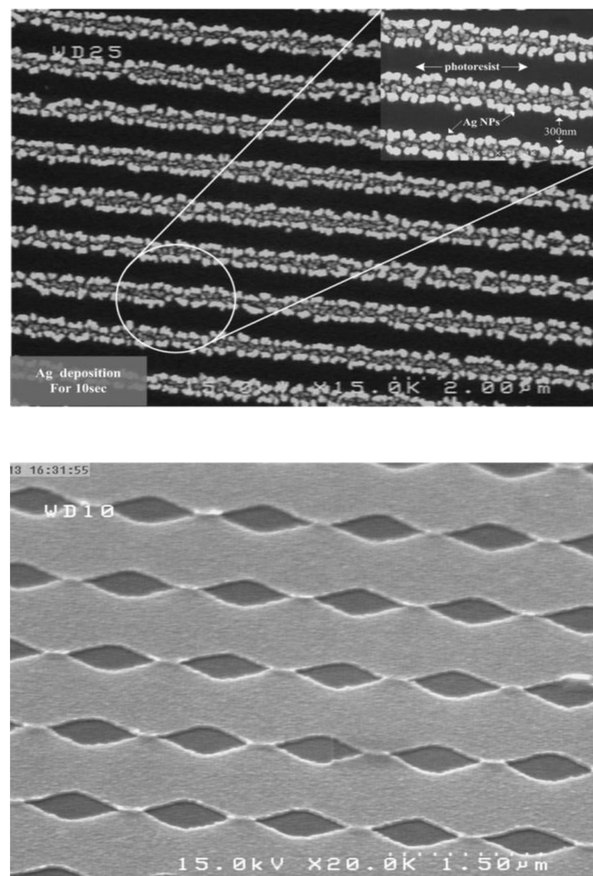

Fig. 2. SEM images of (a) Ag nanoparticles deposited from $AgNO_3$ electroless plating solution, and (b) 30 nm evaporated Ag layer.

As is clear from the images, unlike the evaporated silver layer, the metal distribution does not produce a continuous layer in electroless deposition. This discontinuity is the key factor in the formation of either silicon nanoholes or porous structures. Another notable key factor to this formation is that the metal thickness and deposition rate determines the accessibility of the Si/Metal interface by the etching solution.

It is worth noting that in MaCE, deposited metals are almost inert to HF acid. Therefore, if the thickness of the metal layer exceeds a critical thickness, it will act as a mask for etching. Fig.3(a) and 4(a) show SEM images of the samples that were etched for 10 minutes. The result structure in Fig. 3(a) is rhomboidal shape. The Thickness of the Ag layer for these samples was measured to be 15nm using a HORIBA JobinYvon Ellipsometer.

The reflectance spectrum of Fig. 3(a) is shown in Fig. 3(b). The difference between duty cycles in 2 dimensions of PC can be produced by different exposure doses in 2 dimensions, meaning that the spectrum responses for two polarizations are different.

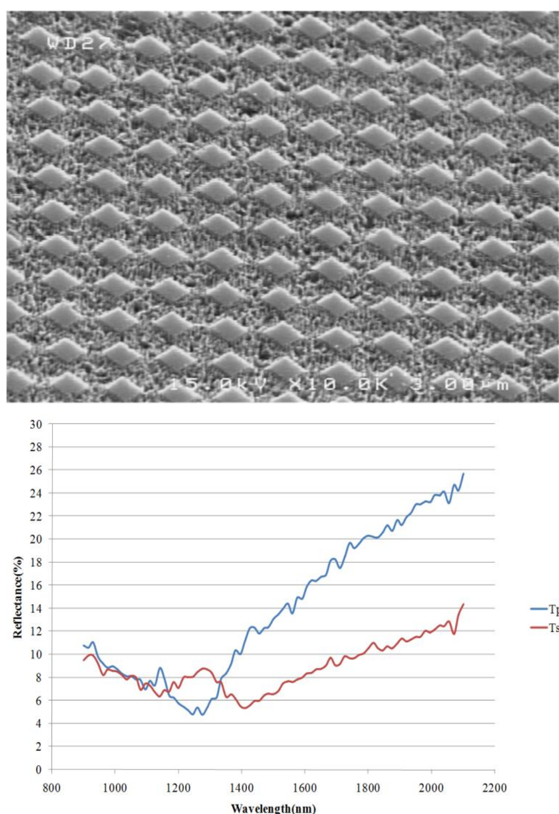

Fig. 3. (a) SEM image of rhomboidal shape sample MaCE and (b) reflection spectra of PC sample for both P and S polarizations.

The patterned region in Fig. 3(a) has a minimum size of 600nm while for Fig. 4(a) this minimum is about 900nm. Porous structures are evident from the SEM images. Such a porous structure directly corresponds to the metal thickness (15nm), where the metal discontinuity leads to the release of the hydrogen gas through the metal voids and the consequently porous structure formation.

Fig. 4(b) and (c) show SEM images of the samples with a 30nm Ag layer deposited over the samples after etching. These two samples were etched for 10 and 15min, respectively. The etching solution used was the same as applied for the sample shown in Fig. 3(a) and 4(a). The result structures are periodic hole arrays that were drilled in vertical direction relative to substrate surface. This effect seems to be associated with increase in the thickness of the Ag layer, as mentioned vide supra. An increase in the thickness of the metal layer will change the etching regime from porous formation to vertical etching of silicon because the hydrogen gas released from the Si/metal interface does not result in metal displacement when the metal layer is continuous.

Reflection spectra of for Fig. 4(a)-(c)are shown in Fig. 4(d). All of these samples that were etched using MaCE, exhibit reflection less than bare silicon (between 30 up 50%, depending on the Si type) in 900 to 2200nm of spectrum. Such structures can be designed to further decrease in the reflection (less than 1%) in the broadband of spectrum by changing the shapes [26], filling factor and depth [27]. From reflectance spectra it is obvious that sample with rod like structure and porous surface (Fig. 4(a)) presents much less reflectance than nanohole array one (Fig. 4(b) and (c)). This could be resulted from combination of light coupling in PC structure and also its entrapment in porous surface while this reflectance

is decreased for sample in Fig. 4(c) compare to Fig. 4(b) because of its deeper nanoholes.

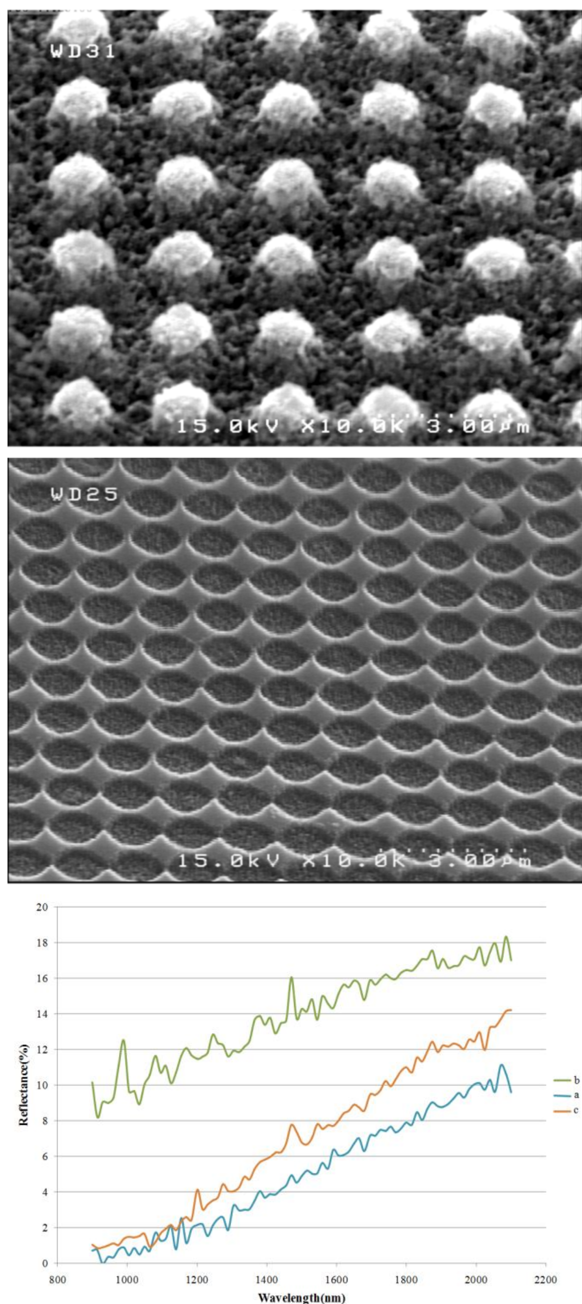

Fig. 4. SEM images of samples (a) with 19 nm Ag layer thickness that was etched for 10 min, and (b) and (c) with a 30 nm Ag layer thickness that were etched 10 min and 15 min respectively. Due to an 11 nm increase in Ag thickness the porous formation regime is changed to vertical etching (Fig 4(d)). Reflection spectra of samples shown in Figures (a), (b) and(c)

In Fig. 4(b) and (c) which the periodic hole array have been fabricated, the reflection spectra are comparable to our previous studies [27, 28], where we used ICP-RIE technique to fabricate silicon nanoholes and nanorods. However, MaCE does not need to complicate process and expensive facilities to achieve such comparable specifications. In the other hand, it can be applied in large area substrate involved in Photovoltaic (PV) device mass production. In addition to lower reflectance, the hole shape structure have more life rather than pillar structure because of its less fragility. Another issue in application of such periodic structure in PV application is making a good contact to these structures. When the depth of holes or height of rods increases, thicker conductive layer is needed to make stable and well-covered contact. Consequently, the reflection from the conductive layer will increase and the overall efficiency will decrease. MaCE presents stable, low depth structures with the same reflectance characteristics achieved by deep holes and long rods which will be more applicable in PV industry.

4. Conclusion

In this research we investigated the metal-assisted chemical etching of silicon. MaCE is an effective method for producing silicon nanostructures. The etching regime can be varied according to the desired application from a porous formation to either SiNW arrays or vertical etching. By controlling the concentration of the etching solution, the thickness and distribution of metal catalyst and the type of metal, all etching regimes can be achieved.

We have shown that combination of LIL and MaCE is a suitable method for fabricating regular arrays of pillars, holes and rhomboidal structures in a high refractive index material to reduce the

reflectance. The reflectance of fabricated PCs depends on their height, pitch, width and shape. MaCE can be applied for large area fabrication in mass production of PV devices, due to its high mechanical stability and low fabrication costs.

Acknowledgment

The financial support of this work by Islamic Azad University, Roudehen branch is gratefully acknowledged.

References

[1] H. Fukuda, K. Yamada, T. Tsuchizawa, T. Watanabe, H. Shinojima, S. Itabashi, Opt. Express 14 (2006) 12401-12408
[2] M. Balucani, V. Bondarenko, N. Vorozov and A. Ferrari, Physica E: Low-dimensional Systems and Nanostructures16 (2003) 586-590
[3] F. Raissi, R. Farivar, Applied Physics Letters 8 (2005)7164101-164101
[4] G. M. O'Halloran, M. Kuhl, P. J. Trimp, P. French, Sensors and Actuators A: Physical 61 (1997) 415-420
[5] L. Tsakalakos, J. Balch, J. Fronheiser, B. A. Korevaar, O. Sulima, J. Rand, Appl. Phys. Lett. 91 (2007) 233117
[6] C. K. Chan, H. Peng, G. Liu, K. Mcilwrath, X. F. Zhang, Nat. Nanotechnol.3 (2008) 31–35
[7] Y. Cui, Z. Zhong, D. Wang, W. U. Wang, C. M. Lieber, Nano Lett.3 (2003) 149
[8] J. Hu, M. Ouyang, P. Yang, C. M. Lieber, Nature 3 (1999) 9948
[9] A. I. Boukai, Y. Bunimovich, J. Tahir-Kheli, J. Yu,W. A. Goddard,J. Heath, Nature 451 (2008) 168
[10] C. M. McAlpine, R. Friedman, S. Jin, K. Lin, W. U. Wang, C. M. Lieber, Nano Lett. 3 (2008) 1531
[11] Y. Huang, X. Duan, C. LieberSmall1 (2005) 142
[12] B. Tian, P. Xie, T. J. Kempa, D. C. Bell, C. M. Lieber, Nat. Nanotechnol.4 (2009) 824
[13] K. Byun, K. Heo, S. Shim, C. Choi, S. Hong, Small 5 (2009) 2659
[14] W. Kim, K. Ng, M.E. Kunitake, B.R Conklin, P. Yang, J. Am. Chem. Soc.129 (2007) 7228
[15] W. Chen, H. Yao, C.H Tzang, J. Zhu, M. Yang, S. Lee, Appl. Phys. Lett.88 (2006) 213104
[16] G. Zheng, F. Patolsky, Y. Cui, W.U. Wang, C.M. Lieber, Nat. Biotechnol.23 (2005) 1294
[17] Z. Li, Y. Chen, X. Li, T.I. Kamins, K. Nauka, R.S. Williams, Nano Lett. 4 (2004) 245
[18] F. Patolsky, G. Zheng, O. Hayden, M. Lakadamyali, X. Zhuang, C.M. Lieber, Proc. Natl. Acad. Sci. 101 (2004) 14017
[19] X. Li, P.W. Bohn, Appl. Phys. Lett.77 (2000) 2572
[20] K. Peng, Y. Wu, H. Fang, X. Zhong, Y. Xu, Zhu J. Angew. Chem. Int. Ed.44 (2005) 2737
[21] M. Zahedinejad, M. Khaje, M. Erfanian, F. Raissi, J. Micromech. Microeng.21 (2011) 065006
[22] C.J.M. Van Rijn, G.J. Veldhuis, S. Kuiper, Nanotechnology9 (1998) 343
[23] V. Berger, O.Gauthier-Lafaye, E. Costard Electron.Lett.33 (1997) 425
[24] S.S. Song, E.U. Kim, H.S. Jung, K.S. Kim, G.Y. Jung, J. Micromech. Microeng.19 (2009) 105022
[25] G. Veronis, R.W. Dutton, S.J. Fan, Appl. Phys. 97 (1997) 093104
[26] S. Dom’inguez, I. Cornago, O. Garc’ia, M. Ezquer, M.J. Rodr’iguez, A.R. Lagunas, J. P’erez-Conde et al. Phot. Nano. Fund. Appl. In press
[27] M. Malekmohammad, M. Soltanolkotabi, A. Erfanian, R. Asadi, S. Bagheri, M. Zahedinejad M. Khaje, et al. J. Europ. Opt. Soc.7 (2012) 12008
[28] M. Malekmohammad, M. Soltanolkotabi, R. Asadi, M.H. Naderi, A. Erfanian, M. Zahedinejad, S. Bagheri, et al. J. Micro/Nanolith. MEMS MOEMS (2012) 013011.
[29] W.K. Choi, T.H. Liew, M.K. Dawood, Nano.Lett.8 (2008) 3800.
[30] C. Kittel, Introduction to Solid State Physics, Wiley, New York, 1983.